Light Scattering and Dielectric Measurements in $(PbMg_{1/3}Nb_{2/3}O_3)_{0.67}(PbTiO_3)_{0.33}$ Single Crystal

V. Hugo Schmidt[1], Chi-Shun Tu[2], C.-H. Yeh[2], H. Luo[3] and F.-C. Chao[2]

[1]*Department of Physics, Montana State University, Bozeman, Montana 59717*
[2]*Department of Physics, Fu Jen University, Taipei 242, Taiwan*
[3]*Laboratory of Functional Inorganic Materials, Shanghai Institute of Ceramics, Chinese Academy of Science, Shanghai 201800, P.R. China.*

Abstract. The longitudinal Brillouin back-scattering spectra, dielectric permittivities and polarization-electric field (P-E) hysteresis loops along the [111] direction have been measured as a function of temperature for a relaxor ferroelectric single crystal $(PbMg_{1/3}Nb_{2/3}O_3)_{0.67}(PbTiO_3)_{0.33}$ (PMN-33%PT). A sharp ferroelectric phase transition, which is associated with a minimum in phonon frequency and an abrupt change in polarization, was observed near 425 K. As temperature decreases, a diffuse phase transition which is associated with a broad frequency-dependent dielectric spectrum and a gradual evolution in polarization, was detected near 350 K. In addition, the nature of the thermal hysteresis for the dielectric permittivity confirms that these transitions (near 350 and 425 K) are diffuse first-order and first-order, respectively. The field-cooled-zero-field-heated dielectric permittivities show that the dc bias field induces a long-range ferroelectric phase transition at 357 K and imply the phase coexistence of a short-range electric ordering and a long-range electric ordering in the region of ~330-380 K.

INTRODUCTION

Relaxor ferroelectrics generally mean the complex ABO_3-type unit cell and are crystals in which unlike-valence cations belonging to a given site (A or B) are present in the correct ratio for charge balance, but are situated randomly on these cation sites. These randomly different cation charges give rise to random fields. These random fields tend to make the phase transitions "diffuse" instead of sharp as in normal ferroelectrics.[1-7] $Pb(Mg_{1/3}Nb_{2/3})O_3$ (PMN) is one of the most interesting relaxor ferroelectric (FE) materials. PMN has a disordered complex structure in which the Mg^{2+} and Nb^{5+} cations exhibit only short range order on the B-site. PMN undergoes a diffuse transition near 280 K and has cubic symmetry at room temperature, whereas below 200 K a small rhombohedral distortion was observed.[1] $PbTiO_3$ (PT) has tetragonal symmetry with space group *P4mm* at room temperature and has a larger tetragonality and a higher FE phase transition temperature (T_c=760 K) compared with those of $BaTiO_3$.[2,3]

The mixed system $(PbMg_{1/3}Nb_{2/3}O_3)_{1-x}(PbTiO_3)_x$ (PMN-*x*PT) naturally has a

morphotropic phase boundary (MPB) [tetragonal FE phase $\leftrightarrow$ rhombohedral FE phase], where huge dielectric and piezoelectric constants appear, as is similar to the case in the $PbZrO_3$-$PbTiO_3$ (PZT) system.[4-5] The piezoelectric constants and the electromechanical coupling factors so far reported for the PMN-*x*PT crystals are larger than those in the PZT family of ceramics.[4-6] Several papers have reported the large piezoelectric constants (d_{33}>1500$\times 10^{-12}$ C/N) and electromechanical coupling parameters (k_{33}>70 %) of PMN-*x*PT based crystals.[4-6] Single crystal growth of PMN-*x*PT by the flux technique is also easier than for PZT which makes PMN-*x*PT a promising material for high-strain transducers. However, the understanding of acoustic phonon and dielectric anomalies near the MPB is still lacking. This motivated us to carry out Brillouin scattering, dielectric permittivity and P-E hysteresis loop measurements on PMN-33%PT. In particulars, direct evidences for successive phase transitions and an acoustic phonon soft mode in PMN-33%PT are presented.

EXPERIMENTAL PROCEDURE

The lead magnesium niobate-lead titanate single crystal PMN-~33%PT was grown by the high temperature flux solution method. The sample was cut perpendicular to the [111] direction. The longitudinal acoustic (LA) phonon spectra were obtained from Brillouin back-scattering. The sample was illuminated along the [111] direction with an *Innova 90 plus-A3* argon laser with wavelength λ=514.5 nm, so the LA phonons with wave vector along [111] direction were studied. Scattered light was analyzed by a Burleigh five-pass Fabry-Perot (F-P) interferometer. The free spectral range (FSR) of the F-P interferometer was determined from measuring the LA phonon frequency shift of fused quartz with a signal/noise (*S/N*) ratio greater than 70. The Brillouin scattering data were taken during a step heating process.

For measurements of dielectric permittivities and P-E hysteresis loop, the sample surfaces were coated with silver paste electrodes. A variable-frequency *Wayne-Kerr Precision Analyzer Model PMA3260A* with four-lead connections was used to obtain capacitance and resistance. The heating/cooling rate for dielectric measurements was 1.5 K/min. For the field-cooled-zero-field-heated (FC-ZFH) dielectric measurement, the sample was first cooled from 470 K through T_c to room temperature with a dc bias field of E=10 kV/cm along the [111] direction. Then the dielectric permittivity of the sample were measured upon heating without a bias field. In the zero-field-heated (ZFH) run, the dielectric permittivities were taken directly upon heating without prior field-cooled treatment. The P-E hysteresis loops were measured by using a Sawyer-Tower circuit in which the P-E hysteresis loop was obtained within 2-3 cycles of electric field at frequency 43 Hz. A *Janis Model CCS-450* closed cycle refrigerator was used with a *Lakeshore Model 340* controller for temperature-dependent measurements.

RESULTS AND DISCUSSION

Figs. 1(a)-1(c) show the temperature dependences of the acoustic phonon

frequency shift, half-width and the real part $\varepsilon'_{<111>}$ of dielectric permittivity at measuring frequency 50 kHz, respectively. Due to the weak intensity factor, and uncertainty of collection angle which can appreciably broaden and distort the Brillouin line shape, both the frequency shift and half-width data (Fig. 1a and 1b) show scatter.

Figs. 2(a) and 2(b) shows the temperature dependences of both the real $\varepsilon'_{<111>}$ and imaginary $\varepsilon''_{<111>}$ parts of the dielectric permittivity for the frequency range 300 Hz-100 kHz upon heating. The inset of Fig. 2(a) shows the reciprocal of $\varepsilon'_{<111>}$ from both cooling and heating runs. Two clear thermal hystereses were observed in the regions of ~260-360 K and ~400-430 K, respectively. These behaviors indicate that these transitions (near 350 and 425 K) are diffuse first-order and nearly typical first-order FE phase transition, respectively. The inset of Fig. 2(b) is an enlargement of $\varepsilon''_{<111>}$ to clarify the dispersion behavior. Compared with $Pb(Mg_{1/3}Nb_{2/3})O_3$ (PMN) crystal which has a diffuse phase transition near 280 K, PMN-33%PT exhibits a narrower frequency dispersion and stronger dielectric maximum near 425 K due to the PT content, though not as sharp as in pure PT. In addition, near 350 K $\varepsilon'_{<111>}$ exhibits a broad weaker plunge accompanied by a dispersion which is usually connected to the diffuse transition.

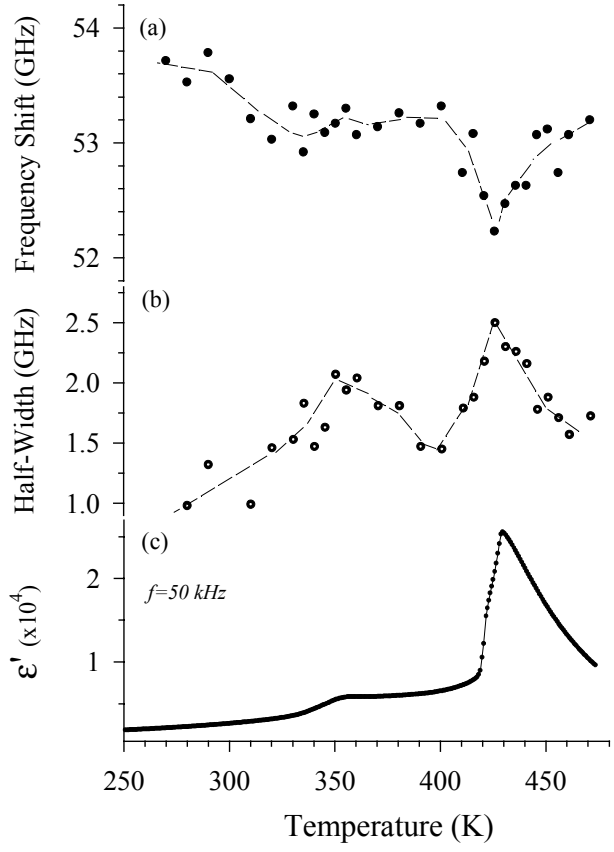

FIGURE 1. (a) Brillouin frequency shift, (b) half-width and (c) the real part $\varepsilon'_{<111>}$ of dielectric permittivity vs. temperature. The dashed lines are guides for the eye.

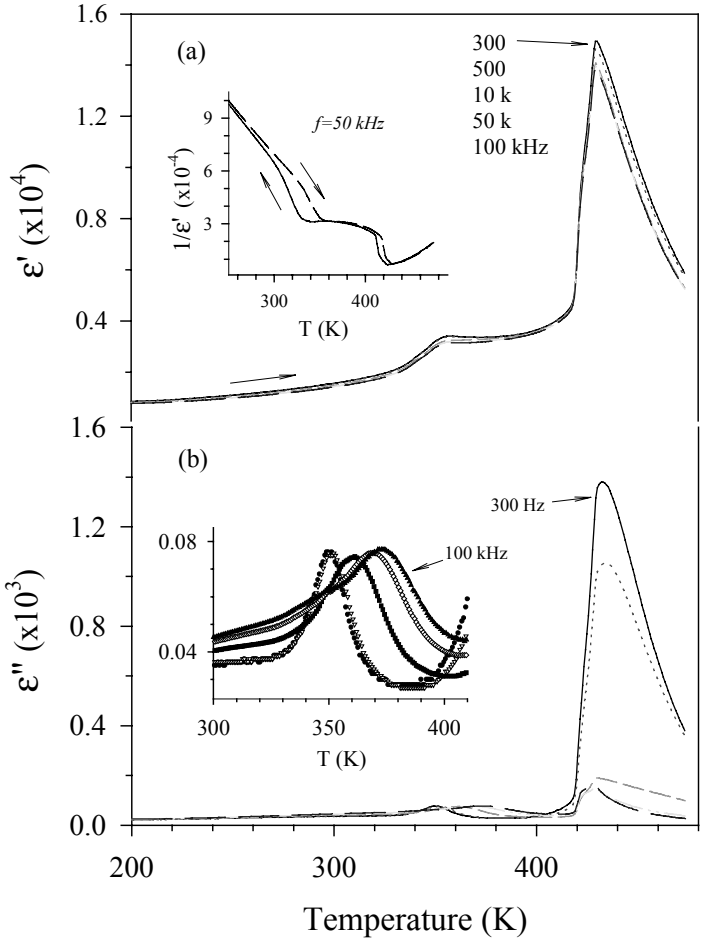

FIGURE 2. Temperature dependences of (a) $\varepsilon'_{<111>}$ and (b) $\varepsilon''_{<111>}$ upon heating. The data were obtained from the ZFH run. The inset of Fig. 2(a) is the reciprocal of $\varepsilon'_{<111>}$ from both cooling and heating runs at measuring frequency f=50 kHz. The inset of Fig. 2(b) is enlargement of $\varepsilon''_{<111>}$.

What are the origins of the temperature-dependent Brillouin spectra and dielectric phenomena shown in Figs. 1 and 2 near 425 K? For a typical FE phase transition, the transition temperature occurs where the frequency shift curve for acoustic phonon has an abrupt change.[8] In PMN-33%PT, the acoustic phonon frequency (Fig. 1a) reaches a sharp turning point near 425 K. In addition, a damping maximum (Fig. 1b) which can be associated with a Landau-Khalatnikov-like maximum, was observed near 425 K. Such a damping anomaly is usually attributed to a rapid growth of long-range electric ordering. The $\varepsilon'_{<111>}$ (Figs. 1c and 2) exhibits a steep change (with narrow frequency dispersion) and an obvious thermal hysteresis near 425 K. Thus, PMN-33%PT single crystal possesses a sharp first-order FE phase transition near 425 K. This value is close to the transition temperature 430 ± 5 K (cubic paraelectric phase $\leftrightarrow$ tetragonal FE phase) predicted from the morphotropic phase boundary in the Ref. 9.

Ferroelectric transitions are known to be associated with a crystal lattice soft mode.

Lines and Glass pointed out that if the transition is strongly first-order, mode softening may not be detectable.[8] Thus, the phase transition near 425 K (paraelectric phase $\leftrightarrow$ FE phase) for PMN-33%PT should be weak first-order. We note that a zone-center (q=0) acoustic soft mode in the reduced Brillouin zone of the reciprocal sublattice always has, for a second-order transition, a zero frequency on approaching T_c from the ordered phase, i.e. $T \rightarrow T_c^-$. Therefore, the nonzero minimum of phonon frequency shift near 425 K implies either a weak first-order transition or that the structural instabilities (as $T \rightarrow T_c^+$) in PMN-33%PT must be associated with a more complicated mode.

In the lower temperature region, $\varepsilon'_{<111>}$ (Figs. 1c and 2) exhibits a gradual change with a notably extensive frequency dispersion (or diffuse phase transition) and an obvious thermal hysteresis. Correspondingly, $\varepsilon''_{<111>}$ also shows a relatively pronounced frequency dispersion in the same temperature region. The acoustic phonon damping (Fig. 1b) exhibits a gradual growth with a maximum located near 350 K. The acoustic phonon frequency (Fig. 1a) reaches a weaker turning point in this region. Such a slowly rising damping anomaly reveals that order parameter fluctuations are the dominant dynamic mechanism. Similar acoustic and dielectric anomalies were seen in other mixed systems such as $Pb(Mg_{1/3}Nb_{2/3})O_3$ (PMN), $(PbZn_{1/3}Nb_{2/3}O_3)_{1-x}(PbTiO_3)_x$ (PZN-xPT) and $Rb_{1-x}(ND_4)_xD_2AsO_4$ (DRADA-x) in which a local short-range order or a coexistence of two different phases were found.[10-12] Near room temperature a dramatic change in the dielectric loss was observed in a PZN-10%PT crystal accompanied by a slight change in the real part of dielectric permittivity.[3] The previous X-ray diffraction data of the PZN-10%PT crystal also evidenced a mixed phase of rhombohedral and tetragonal symmetries at the morphotropic phase boundary.[3] In the supposedly disordered PMN crystal, a nanometric microstructure with 1:1 (B':B") cation ordering was reported.[13,14] Such 1:1 ordering, when charge naturally requires 1:2 stoichiometry, implies locally charged regions causing fields which can induce order parameter fluctuations. Thus, the diffuse phase transition near 350 K could be triggered by the local structural fluctuations, perhaps between rhombohedral and tetragonal symmetries. We call this a first-order transition only because the thermal hysteresis in the permittivity shows that the system is metastable in this temperature region. The usual distinctions between first- and second-order transitions, such as discontinuity in dP/dT, do not apply for diffuse transitions.

Fig. 3 shows the temperature dependences of $\varepsilon'_{<111>}$ and $\varepsilon''_{<111>}$ from the field-cooled-zero-field-heated (FC-ZFH) run. Compared to the ZFH run (Fig. 2), the maximum values (near 425K) of $\varepsilon'_{<111>}$ in the FC-ZFH run were reduced about 45%. In addition, near 357 K another sharp transition which is independent of frequency, was observed in both $\varepsilon'_{<111>}$ and $\varepsilon''_{<111>}$. For the FC-ZFH measurement, the sample was first cooled from paraelectric phase to FE ordering with a dc bias field of E=10 kV/cm along the [111] direction. Thus, the reduction of maximum values in $\varepsilon'_{<111>}$ (FC-ZFH) could be associated with the enhancement of the domains polarized along the [111] direction, which is not the preferred polar axis for $PbTiO_3$ (PT) single crystal in the tetragonal symmetry. Hereafter, we use $\varepsilon_{<111>}$(ZFH) and $\varepsilon_{<111>}$(FC-ZFH) to represent the data obtained from the ZFH and FC-ZFH runs, respectively.

Fig. 4 shows the comparison of $\varepsilon''_{<111>}$(FC-ZFH) and $\varepsilon''_{<111>}$(ZFH) in the region 270-410 K. The composite shapes of $\varepsilon''_{<111>}$(FC-ZFH) are narrower than those in $\varepsilon''_{<111>}$(ZFH). In addition, both $\varepsilon'_{<111>}$ and $\varepsilon''_{<111>}$ in the FC-ZFH run, exhibit a sharp change at 357 K. It was found that the temperature for this anomaly (but not its amplitude) is independent of frequency. Similar anomalies have been seen in the PMN and $Pb_{1-x}La_x(Zr_yTi_{1-y})_{1-x/4}O_3$ (PLZT) relaxor systems from FC-ZFH dielectric measurements.[15,I6] By cooling the PMN crystal in a dc electric field higher than the critical field $E_c \approx 1.7$ kV/cm, the establishment of long-range ferroelectric order is evidenced in the FC-ZFH procedure.[15] It was concluded that the less diffuse behavior with little frequency dispersion is due to macro-domain pinning which can greatly reduce relaxor-type behavior.[9] Thus, the sharp transition at 357 K implies a development of long-range ferroelectric ordering.

The temperature-dependent composite shapes of $\varepsilon''_{<111>}$(ZFH) imply that two kinds of mechanisms could be involved in the diffuse phase transition region (~320-400 K). To check this, the experimental results were fitted to two Lorentz functions;

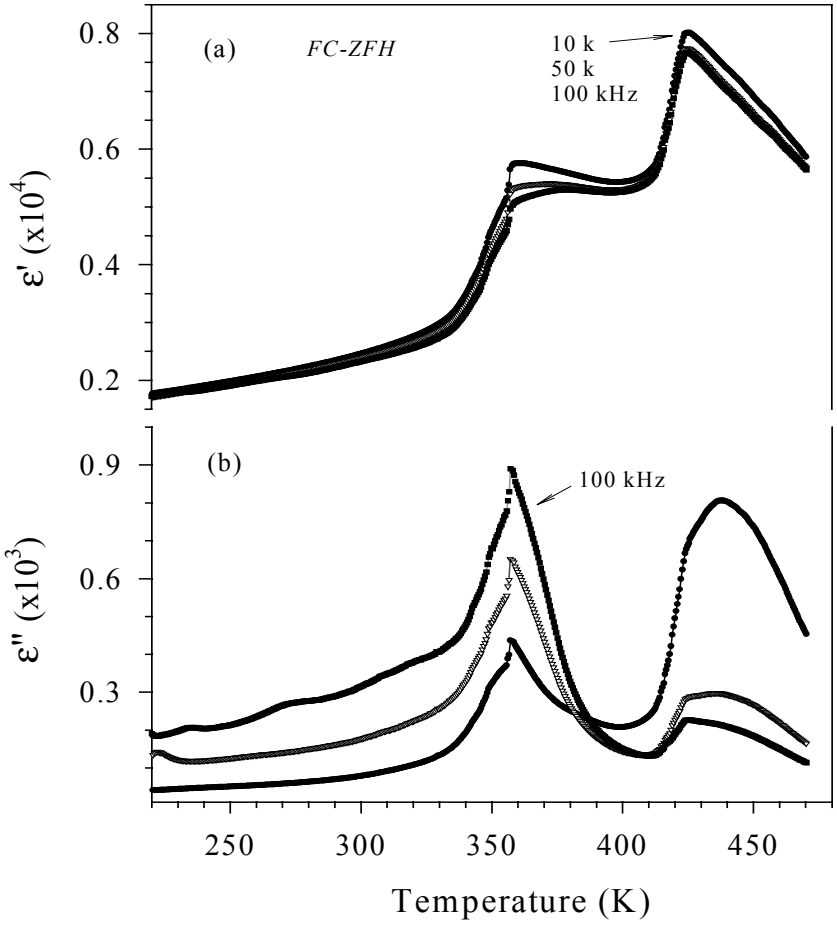

FIGURE 3. Temperature dependences of (a) $\varepsilon'_{<111>}$ and (b) $\varepsilon''_{<111>}$ obtained from the FC-ZFH run.

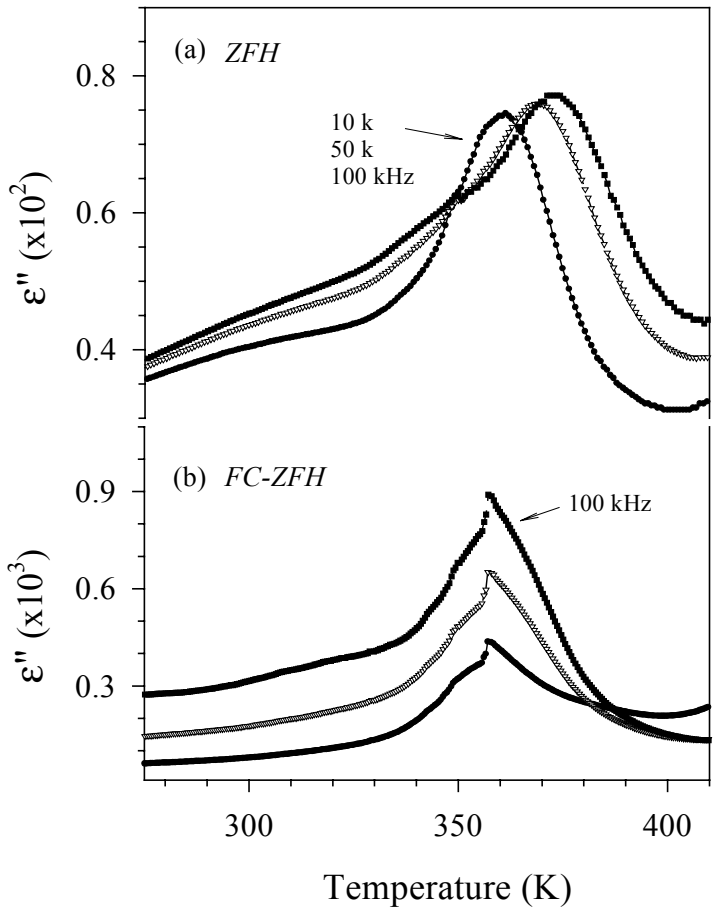

FIGURE 4. Comparison of $\varepsilon''_{<111>}$(ZFH) and $\varepsilon''_{<111>}$(FC-ZFH) in the region of 270-410 K.

$$\varepsilon''_{<111>}(T) = A\{1+[(T-T_{gI})/\Delta_I]^2\}^{-1} + B\{1+[(T-T_{gII})/\Delta_{II}]^2\}^{-1} \quad (1)$$

where T_{gI} and T_{gII} are temperatures corresponding to the peaks in $\varepsilon''_{<111>}$(ZFH) near 360 K. Figure 5(a) illustrates the best fits for measuring frequency 100 kHz. The maximum positions of these two peaks were found to be frequency-dependent. This phenomenon may imply a mixed phase of two different structures, perhaps rhombohedral and tetragonal symmetries. However, the composite shapes of $\varepsilon''_{<111>}$(FC-ZFH) cannot be fitted with two Lorentz functions. Fig. 5(b) illustrates the best fits with three Lorentz functions for measuring frequency 100 kHz. Whereas the maximum positions of peaks II and III were found to be frequency-dependent, peak I (located at 357 K) is independent of frequency. With the sharp transition near 357 K in $\varepsilon'_{<111>}$ (FC-ZFH), one can expect that peak I is associated with the establishment of long-range ferroelectric ordering. On the whole, the FC-ZFH dielectric data implies a phase coexistence of short-range electric ordering (which is responsible for the frequency-dependent behaviors), and long-range electric ordering (which causes the frequency-independent transition near 357 K) in the region of 320-380 K.

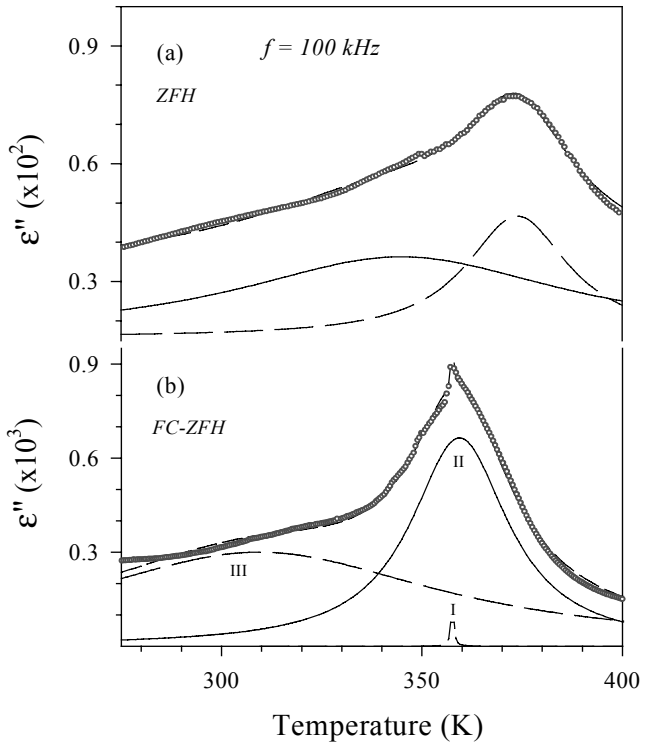

FIGURE 5. Illustration of the best fits with (a) two Lorentz functions for $\varepsilon''_{<111>}$ (ZFH) and (b) three Lorentz functions for $\varepsilon''_{<111>}$ (FC-ZFH). The data were taken at measuring frequency 100 kHz.

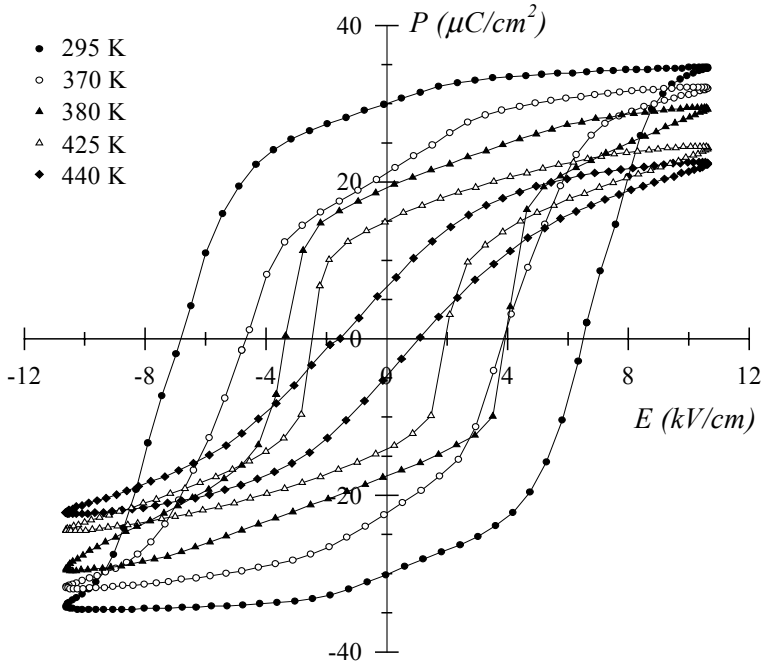

FIGURE 6. P-E hysteresis loops for various temperatures.

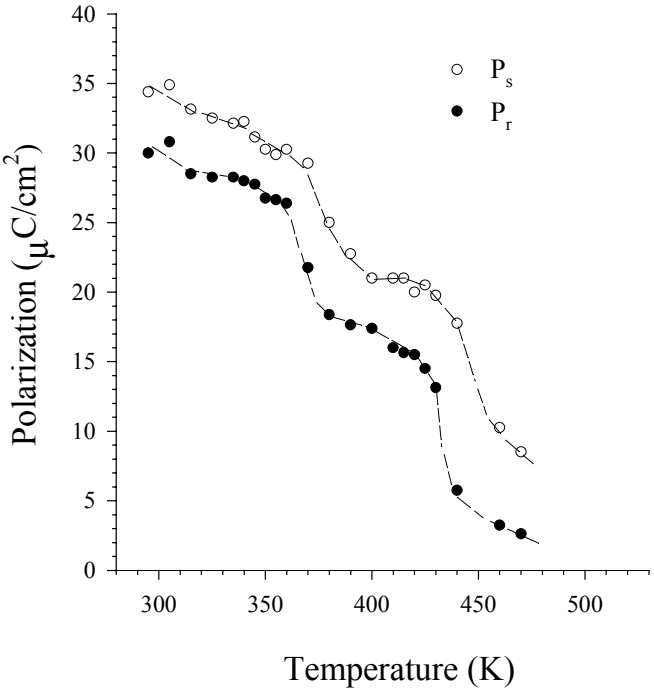

FIGURE 7. Temperature dependence of apparent spontaneous (P_s) and remanent (P_r) polarizations along a pseudocubic <111> direction. The dashed lines are guides for the eye.

Fig. 6 shows P-E hysteresis loops for various temperatures near transitions. The temperature-dependent spontaneous and remanent polarizations are plotted in Fig. 7. At room temperature, the spontaneous P_s and remanent P_r polarizations are about 34 $\mu C/cm^2$ and 30 $\mu C/cm^2$, respectively. Compared with $PbMg_{1/3}Nb_{2/3}O_3$ (PMN),[2] PMN-33%PT has a larger value of spontaneous polarization because $PbTiO_3$ has larger tetragonality and P_s (>50 $\mu C/cm^2$).[17,18] An abrupt step-like change in both spontaneous and remanent polarizations was observed near 425 K, which confirm a first-order phase transition. Near 350 K, both P_s and P_r exhibit a gradual temperature-dependent evolution. A similar polarization anomaly was seen in $Pb(Mg_{1/3}Nb_{2/3})O_3$ single crystal.[2] This behavior suggests a diffuse phase transition taking place in this temperature region.

CONCLUSIONS

From the temperature-dependent LA[111] Brillouin scattering spectra, dielectric permittivities ($\varepsilon'_{<111>}$ and $\varepsilon''_{<111>}$) and P-E hysteresis loops of PMN-33%PT, two successive phase transitions are evidenced near 425 K (paraelectric phase $\leftrightarrow$ FE phase) and 350 K (a diffuse transition), respectively. The diffuse phase transition which was observed near 350 K is associated with a broad frequency-dependent dielectric spectrum and a gradual evolution in polarization. The local structural fluctuation

between rhombohedral and tetragonal symmetries is responsible for the development of the diffuse phase transition. In addition, the nature of the thermal hysteresis for the dielectric permittivity confirms that these transitions (near 350 and 425 K) are diffuse first-order and first-order, respectively.

From the FC-ZFH dielectric measurements, one sharp phase transition was evidenced at 357 K due to the establishment of a long-range ordering. Near 425 K, the phase transition (cubic paraelectric phase $\leftrightarrow$ tetragonal FE phase) showed a weaker dielectric peak, probably because of a different tetragonal phase domain pattern resulting from the electric poling procedure.

ACKNOWLEDGMENTS

This work was supported by DOD EPSCOR Grant No. N00014-99-1-0523 and Grant No. NSC89-2112-M-030-003 of National Science Council (Republic of China).

REFERENCES

1. L.A. Shebanov. P. Kaspostins, and J. Zvirgzds, Ferroelectrics **56**, 1057 (1984).
2. V.A. Bokov and I.E. Mylnikov, Soviet Physics-Solid State **3**, 613 (1961).
3. M.L. Mulvihill, S.E. Park, G. Risch, Z. Li, and K. Uchino, Jpn. J. Applied Phys. **35** (part 1), 3984 (1996).
4. S.-E. Paek and T.R. Shrout, J. Appl. Phys. **82**, 1804 (1997).
5. Y. Yamashita, Jpn J. Appl. Phys. **33** (part 1), 5328 (1994).
6. S.W. Choi, T.R. Shrout, S.J. Jang and A.S. Bhalla, Ferroelectrics **100**, 29 (1989).
7. J. Kuwata, K. Uchino and S. Nomura, Jpn. J. Applied Phys. **21**, 1298 (1982).
8. M.E. Lines and A.M. Glass, *Principles and Applications of Ferroelectrics and Related Materials*, (Oxford, London, 1977).
9. T.R. Shrout, Z.P. Chang, N. Kim, and S. Markgraf, Ferroelectrics Letters **12**, 63 (1990).
10. C.-S. Tu, V.H. Schmidt, and I.G. Siny, J. Appl. Phys. **78**, 5665 (1995).
11. C.-S. Tu and V.H. Schmidt, Phys. Rev. B **50**, 16167 (1994).
12. C.-S. Tu, F.-C. Chao, C.-H. Yeh, C.-L. Tsai, and V. H. Schmidt, Phys. Rev. B **60**, 6348 (1999).
13. A.D. Hilton, D.J. Barber, C.A. Randall, and T.R. Shrout, J. Mater. Sci. **25**, 3461 (1990).
14. S.B. Vakhrushev, A.A. Nabereznov, Y.P. Feng, S.K. Sinha, S.M. Shapiro, T. Egami, H.D. Rosenfeld, and D.E. Moncton, Bull. Am. Phys. Soc. **39**, 680 (1994).
15. R. Sommer, N.K. Yushin, and J.J. van der Klink, Phys. Rev. B **48**, 13230 (1993).
16. V. Bobnar, Z. Kutnjak, R. Pirc, and A. Levstik, Phys. Rev. B **60**, 6420 (1999).
17. G. Shirane, S. Hoshino and K. Suzuki, Phys. Rev. **80**, 1105 (1950).
18. E.C. Subbarao, Ferroelectrics **5**, 267 (1973).